European Journal of Control 68 (2022) 100693

Contents lists available at ScienceDirect

European Journal of Control

journal homepage: www.elsevier.com/locate/ejcon

Rolling horizon games of resilient networks with non-uniform horizons☆

Yurid Nugraha[a], Ahmet Cetinkaya[b], Tomohisa Hayakawa[a,*], Hideaki Ishii[c], Quanyan Zhu[d]

[a] Department of Systems and Control Engineering, Tokyo Institute of Technology, Tokyo 152-8552, Japan
[b] Department of Functional Control Systems, Shibaura Institute of Technology, Tokyo 135-8548, Japan
[c] Department of Computer Science, Tokyo Institute of Technology, Yokohama 226-8502, Japan
[d] Department of Electrical and Computer Engineering, New York University, Brooklyn, NY 11201, USA

ARTICLE INFO

Article history:
Received 18 April 2022
Accepted 6 June 2022
Available online 16 June 2022

Recommended by Prof. T Parisini

Keywords:
Resilient network systems
Game theory
Cybersecurity
Rolling horizon approach

ABSTRACT

A two-player game-theoretic problem on resilient graphs is formulated. An attacker is capable to disable some of the edges of the network with the objective to divide the agents into clusters by emitting jamming signals while, in response, the defender recovers some of the edges by increasing the transmission power for the communication signals. We consider repeated games between the attacker and the defender where the optimal strategies for the two players are derived in a rolling horizon fashion by taking account of the sizes of the clusters. The players' actions at each discrete-time step are constrained by their energy for transmissions of signals. We derive several theoretical results to characterize the properties of the two-player game under some specific conditions of the agents' communication network and the players' energy parameters. In order to investigate more general cases, we provide some numerical evaluations to show the effects of the values of horizon lengths and game periods on the players' performance.

1. Introduction

Networked systems have been used in various areas of critical infrastructures including power grids and transportation systems. While wireless communication among agents plays an important role for the functionality of the network, it is also prone to cyber attacks initiated by malicious adversaries [1,6,16]. Attacks on cyber-physical systems can result in not only damages in equipments but also serious accidents in worst cases, and hence are considered as a major threat to the society.

From such perspectives, security issues in multiagent systems have gained much attention. Jamming attacks on consensus problems of multiagent systems have been studied in [2,18]. Noncooperative games between the attacker and another player protecting the network are widely used to analyze security problems, including jamming attacks and injection attacks [7,15]. In the face of the malicious adversaries, agents with consensus protocols may not be able to converge; instead, they are divided into clusters, i.e., groups of agents. Cluster forming in multiagent systems has been studied in, e.g., [14,19], where the relations among certain agents may be hostile.

Receding/rolling horizon control has been employed to deal with multiagent systems with uncertainties and state constraints. It is used for achieving consensus of a linear multiagent system [9]. It is also studied in noncooperative security game settings in [21], where horizon lengths affect the resilience of the system. Rolling horizon approach has also been followed to obtain better planning, e.g., in an agent with obstacle avoidance constraints [17] and in a multivehicle competitive scenarios for self-driving cars [20].

In this paper, we consider a security problem in a two-player game setting between an attacker, who is motivated to disrupt the communication among agents by attacking communication links, and a defender, who attempts to recover some of the attacked links. This game is played repeatedly over discrete time where the players recalculate and may change their strategies as time goes on, according to the rolling horizon approach. The players' utilities are determined by how agents are divided into clusters.

We formulate the problem based on [4,12], which use graph connectivity to characterize the game and players' strategies.

☆ This work was supported by JST ERATO HASUO Metamathematics for Systems Design Project under Grant JPMJER1603, JSPS KAKENHI under Grants 18H01460, 20K14771, 21K04117, and the National Science Foundation (NSF) under Grant ECCS-1847056.

* Corresponding author.
E-mail addresses: yurid@dsl.sc.e.titech.ac.jp (Y. Nugraha), ahmet@shibaura-it.ac.jp (A. Cetinkaya), hayakawa@sc.e.titech.ac.jp (T. Hayakawa), ishii@c.titech.ac.jp (H. Ishii), quanyan.zhu@nyu.edu (Q. Zhu).

https://doi.org/10.1016/j.ejcon.2022.100693
0947-3580/

Specifically, we address how clusters among agents may form in this security game setting. In this paper, we approach clustering from a viewpoint based on a game-theoretic formulation. This approach can be related to the concept of network effect/externality [8], where the utility of an agent in a certain cluster depends on how many other agents belong to that particular cluster. Such concepts have been used to analyze grouping of agents on, e.g., social networks and computer networks, as discussed in [5,10].

Moreover, in comparison to [4,12], which discuss a single-step two-player attack recovery game in networks, our contributions can be stated as follows: (i) we consider the game which consists of multiple attack-recovery actions, resulting in more complicated strategies; (ii) we consider a rolling horizon approach for the players so that their strategies may be modified as they obtain new knowledge of the system each time; and (iii) we consider the difference in the capabilities of the players, represented by non-uniform values of horizon parameters.

Here we focus on evaluating the players' performance given different computational resources represented by *horizon lengths* (how long in the future the players can plan their strategies) and *game periods* (how long the players apply the obtained strategies without updating). It is expected that the players with longer horizon lengths and shorter game periods perform better over time. The related cases where the players have the same ability to compute their strategies in future time are discussed in [11,13].

The paper is organized as follows. In Section 2, we describe the general problem formulation of the attack-recovery sequence. We then specify the non-uniform horizon length approach for games played over time in Section 3 and discuss some theoretical results in Section 4. We then continue by discussing the formulations with non-uniform game periods in Section 5. The simulation results and conclusion are provided in Sections 6 and 7, respectively.

The notations used throughout this paper are fairly standard in regard to mathematical representations. We denote $|\cdot|$ as the cardinality of a set. The floor function is denoted by $\lfloor\cdot\rfloor$. The sets of positive and nonnegative integers are denoted by $\mathbb{N}$ and $\mathbb{N}_0$, respectively. Furthermore, in regard to the representations associated with players' actions and parameters, we put superscripts A and D to denote the attacker and the defender, respectively, and we put * and $'$ to denote optimal strategies in some different aspects. On the other hand, subscripts of some notations indicate time indices.

2. Problem formulation

We explore a multiagent system of n agents communicating to each other in the face of jamming attacks. The network topology for the normal operation is given by an undirected and connected graph $\mathcal{G} = (\mathcal{V}, \mathcal{E})$. The case where the network topology is given by a directed graph can be similarly handled. The graph consists of the set $\mathcal{V}$ of vertices representing the agents and the set $\mathcal{E} \subseteq \mathcal{V} \times \mathcal{V}$ of edges representing the communication links.

The attacker is capable to block the communication by jamming some targeted edges, represented by the removal of edges in $\mathcal{G}$. On the other hand, we suppose that there is a defender that has the capability to maintain the communication among the agents, e.g., by asking agents to send even stronger communication signals to overcome the jamming signals. These are represented by the action of rebuilding some of the attacked edges.

From this occurence of attacks and recoveries, we characterize the attack-recovery process as a two-player game between the attacker and the defender in terms of the communication among the agents of the network. In other words, we may say that the graphs characterizing the networked system are *resilient* if the group of agents is able to recover from the damages caused by the attacker. However, there may be cases where the resiliency of the graph is reduced due to the stronger attack signals. In this paper, we consider the case where the attacker has two types of jamming signals in terms of their strength, *strong* and *normal*. The defender is able to recover only the edges that are attacked with normal strength. In the following subsections, we first describe the order of attack and recovery actions in one sequence and characterize some constraints that we impose as well as the objective of the problem.

2.1. Attack-recovery sequence

In our setting, the players make their attack/recovery actions at every discrete time $k \in \mathbb{N}_0$. Recall that the underlying, attack-free topology of the multiagent system is represented by $\mathcal{G}$. At time k, the players decide to attack/recover certain edges in the two stages, with the attacker acting first, followed by the defender. Specifically, at time k the attacker attacks $\mathcal{G}$ by deleting $\mathcal{E}_k^{\mathrm{A}} \subseteq \mathcal{E}$ with normal jamming signals and $\overline{\mathcal{E}}_k^{\mathrm{A}} \subseteq \mathcal{E}$ with strong jamming signals with $\mathcal{E}_k^{\mathrm{A}} \cap \overline{\mathcal{E}}_k^{\mathrm{A}} = \emptyset$, whereas the defender recovers $\mathcal{E}_k^{\mathrm{D}} \subseteq \mathcal{E}$. Due to the attacks and then the recoveries at time k, the network changes from $\mathcal{G}$ to $\mathcal{G}_k^{\mathrm{A}} := (\mathcal{V}, \mathcal{E} \setminus (\mathcal{E}_k^{\mathrm{A}} \cup \overline{\mathcal{E}}_k^{\mathrm{A}}))$ and further to $\mathcal{G}_k^{\mathrm{D}} := (\mathcal{V}, (\mathcal{E} \setminus (\mathcal{E}_k^{\mathrm{A}} \cup \overline{\mathcal{E}}_k^{\mathrm{A}})) \cup (\mathcal{E}_k^{\mathrm{D}} \cap \mathcal{E}_k^{\mathrm{A}}))$.

In this paper, we formulate the game where the players attempt to choose the best strategies in terms of edges attacked/recovered to maximize their own utility functions. With $l \in \mathbb{N}$, here the lth game is defined over the horizon of h^{A} and h^{D} steps for the attacker and the defender, respectively, and played every T steps of game period from time $(l-1)T$ to $(l-1)T + \max\{h^{\mathrm{A}}, h^{\mathrm{D}}\} - 1$. Since the game period should be within the horizon, we assume that $1 \le T \le \min\{h^{\mathrm{A}}, h^{\mathrm{D}}\}$. The players make decisions in a rolling horizon fashion as explained more in Section 3; the optimal strategies obtained at $(l-1)T$ for the future time may change when the players recalculate their strategies at the future time lT. Fig. 1 illustrates the discussed rolling horizon game over time; the filled circles indicate the applied strategies and the empty circles indicate the strategies of the game that are discarded.

When a player has a longer horizon length, it indicates that it has a better computational ability relative to its opponent, since the computational burden is directly related to the horizon length (explained in Section 3 later). It is expected that the player with a longer horizon length can perform better in general. This topic on the relationship between the ability of players to calculate several strategies in the future and their performance is discussed, e.g., in chess, where better players search for a move more extensively and deeply [3].

2.2. Energy constraints

The actions of the attacker and the defender are affected by the constraints on the energy availability, which is assumed in this paper to increase linearly in time; furthermore, the energy consumed by the players is proportional to the number of attacked/recovered edges. Here we suppose that the players initially possess certain amount of energy κ^{A} and κ^{D} for the attacker and the defender, respectively. Furthermore, the players' energy supply rates are limited by the constant values of ρ^{A} and ρ^{D} every discrete time step. For example, this models devices which are able to supply energy wirelessly to obstruct/retain communication signals between the agents.

Recall that the attacker has two types of jamming signals, strong and normal. Here, the strong attacks on $\overline{\mathcal{E}}_k^{\mathrm{A}}$ take $\overline{\beta}^{\mathrm{A}} > 0$ energy per edge per unit time compared to the normal attacks on $\mathcal{E}_k^{\mathrm{A}}$, which take $\beta^{\mathrm{A}} > 0$ where $\overline{\beta}^{\mathrm{A}} > \beta^{\mathrm{A}}$. The total energy used by the attacker is constrained as

$$\sum_{m=0}^{k} (\overline{\beta}^{\mathrm{A}} |\overline{\mathcal{E}}_m^{\mathrm{A}}| + \beta^{\mathrm{A}} |\mathcal{E}_m^{\mathrm{A}}|) \le \kappa^{\mathrm{A}} + \rho^{\mathrm{A}} k \tag{1}$$

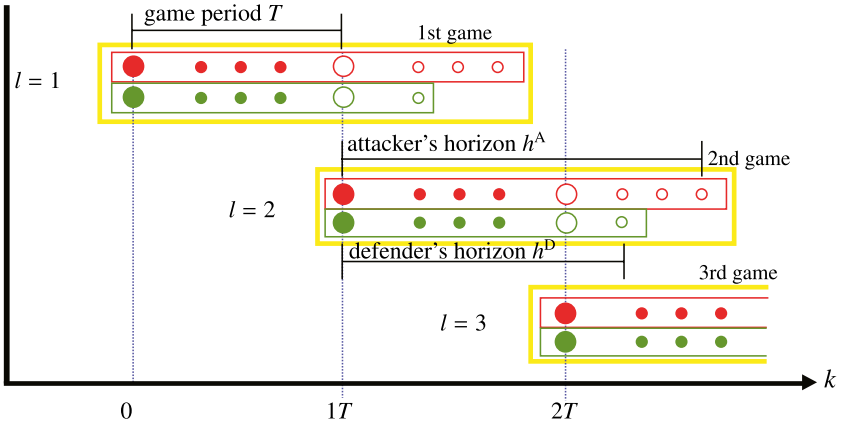

Fig. 1. Illustration of the games played over discrete time k with rolling horizon approach for the players, where the players have different horizon lengths h^{A} and h^{D}.

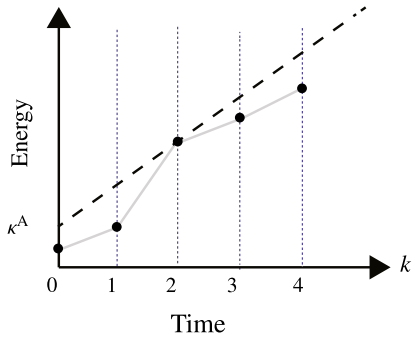

Fig. 2. Energy constraint of the attacker considered in the formulation. The dashed line represents the allowable energy to spend. The solid circles representing the applied energy consumed by the player should be below the dashed line.

for any time k, where $\kappa^{\mathrm{A}} \geq \rho^{\mathrm{A}} > 0$. The energy constraint (1) implies that the total energy spent by the attacker cannot exceed the available energy characterized by the initial energy κ^{A} and the supplied energy $\rho^{\mathrm{A}}k$ by time k. This energy constraint restricts and upper bounds the number of edges that the attacker can attack. See also [2,18] and the references therein for other contraint-based attack models.

Fig. 2 illustrates the energy constraint of the attacker, where the dashed line with slope ρ^{A} represents the total energy supplied and the filled circles indicate the accumulated energy spent. A critical case is when $\beta^{\mathrm{A}} \leq \rho^{\mathrm{A}}$ since it is then possible for the attacker to attack at least one edge for infinite time.

The energy constraint of the defender, which is similar to (1), is given by

$$\sum_{m=0}^{k} \beta^{\mathrm{D}} |\mathcal{E}_m^{\mathrm{D}} \cap \mathcal{E}_m^{\mathrm{A}}| \leq \kappa^{\mathrm{D}} + \rho^{\mathrm{D}} k \tag{2}$$

with $\kappa^{\mathrm{D}} \geq \rho^{\mathrm{D}} > 0$, $\beta^{\mathrm{D}} > 0$. Recall that the defender can recover only the edges in $\mathcal{E}_k^{\mathrm{A}}$ under normal jamming attacks.

2.3. Agents clustering

By attacking, the attacker makes the graph disconnected and separates the agents into clusters (i.e., sets of agents). We introduce a few notions related to grouping/clustering of agents. For a given subgraph $\mathcal{G}' = (\mathcal{V}, \mathcal{E}')$ where $\mathcal{E}' \subseteq \mathcal{E}$, we say that the agents are grouped into $\overline{n}(\mathcal{G}')$ number of *groups*, if the sets of agents $\mathcal{V}_1', \mathcal{V}_2', \ldots, \mathcal{V}_{\overline{n}(\mathcal{G}')}' \subseteq \mathcal{V}$ satisfy $\cup_{a=1}^{\overline{n}(\mathcal{G}')} \mathcal{V}_a' = \mathcal{V}$ and $\mathcal{V}_a' \cap \mathcal{V}_b' = \emptyset$ if $a \neq b$. There is no edge connecting different groups, i.e., $e_{ij} \notin \mathcal{E}'$ for $i \in \mathcal{V}_a'$, $j \in \mathcal{V}_b'$.

Here, we are interested in the case where the attacker is also concerned about the number of agents in each group, as an extension of [12]. Specifically, we follow the notion of *network effect/externality* [8], where the utility of an agent in a certain cluster depends on how many other agents belong to that particular cluster. In the context of this game, the attacker wants to isolate agents so that fewer agents are in each group, while the defender wants as many agents as possible in the same group. We then represent the level of clustering in the graph $\mathcal{G}'$ by the function $c(\cdot)$ called *agent-group distribution*, which is given by

$$c(\mathcal{G}') := \sum_{a=1}^{\overline{n}(\mathcal{G}')} |\mathcal{V}_a'|^2 - |\mathcal{V}|^2. \tag{3}$$

Note that $c(\mathcal{G}')$ is always negative when $\mathcal{G}'$ is disconnected, whereas $c(\mathcal{G}') = 0$ if $\mathcal{G}'$ remains connected.

The attacker and the defender's utility functions of the lth game (lth decision-making opportunity), $l \in \mathbb{N}$, starting at time $k = (l-1)T$, take account of the agent-group distribution $c(\cdot)$ over time horizons $h^{\mathrm{A}}, h^{\mathrm{D}} \geq 1$ from time $(l-1)T$ to $(l-1)T + \max\{h^{\mathrm{A}}, h^{\mathrm{D}}\} - 1$. Specifically, the utility functions at the lth game are defined by

$$U_l^{\mathrm{A}} := \sum_{k=(l-1)T}^{(l-1)T+h^{\mathrm{A}}-1} -c(\mathcal{G}_k^{\mathrm{D}}), \tag{4}$$

$$U_l^{\mathrm{D}} := \sum_{k=(l-1)T}^{(l-1)T+h^{\mathrm{D}}-1} c(\mathcal{G}_k^{\mathrm{D}}). \tag{5}$$

With the rolling horizon approach, the players will be able to manage the usage of their energy better. The player with a longer horizon length is expected to use their energy more efficiently, and thus obtain a higher utility over time.

3. Game structure with non-uniform rolling horizon lengths

We are interested in finding the subgame perfect equilibrium of this game. To find the equilibrium, the game is divided into some subgames/decision-making points. The subgame perfect equilibrium must be an equilibrium in every subgame. The optimal strategy of each player is obtained by using a backward induction approach, i.e., by finding the equilibrium from the smallest subgames. The tie-break condition happens when the players' strategies result in the same utility. In this case, we suppose that the players choose to save their energy by attacking/recovering less edges; otherwise, i.e., they have enough energy to attack/recover all edges in every subsequent steps, then they will attack/recover more edges, given the same resulting utility.

In this paper we consider the situation where the attacker and the defender have different horizon lengths denoted by h^{A} and h^{D}, respectively. The difference in the horizon lengths corresponds to the different ability of the players to solve the game.

Due to the nature of the rolling horizon approach, the strategies obtained for the lth game, i.e., attacked and recovered edges, are applied only from time $(l-1)T$ to $lT-1$ with $T \leq \min\{h^{\mathrm{A}}, h^{\mathrm{D}}\}$. Note that T is set to be the same for the players. The players' strategies at the lth game are specified as $((\bar{\mathcal{E}}^{\mathrm{A}}_{l,1}, \mathcal{E}^{\mathrm{A}}_{l,1}, \mathcal{E}^{\mathrm{D}}_{l,1}), \ldots, (\bar{\mathcal{E}}^{\mathrm{A}}_{l,h^{\mathrm{D}}}, \mathcal{E}^{\mathrm{A}}_{l,h^{\mathrm{D}}}, \mathcal{E}^{\mathrm{D}}_{l,h^{\mathrm{D}}}), (\bar{\mathcal{E}}^{\mathrm{A}}_{l,h^{\mathrm{D}}+1}, \mathcal{E}^{\mathrm{A}}_{l,h^{\mathrm{D}}+1}), \ldots, (\bar{\mathcal{E}}^{\mathrm{A}}_{l,h^{\mathrm{A}}}, \mathcal{E}^{\mathrm{A}}_{l,h^{\mathrm{A}}}))$ if $h^{\mathrm{A}} > h^{\mathrm{D}}$, and $((\bar{\mathcal{E}}^{\mathrm{A}}_{l,1}, \mathcal{E}^{\mathrm{A}}_{l,1}, \mathcal{E}^{\mathrm{D}}_{l,1}), \ldots, (\bar{\mathcal{E}}^{\mathrm{A}}_{l,h^{\mathrm{A}}}, \mathcal{E}^{\mathrm{A}}_{l,h^{\mathrm{A}}}, \mathcal{E}^{\mathrm{D}}_{l,h^{\mathrm{A}}}), \mathcal{E}^{\mathrm{D}}_{l,h^{\mathrm{A}}+1}, \ldots, \mathcal{E}^{\mathrm{D}}_{l,h^{\mathrm{D}}})$ if $h^{\mathrm{A}} < h^{\mathrm{D}}$, with $\bar{\mathcal{E}}^{\mathrm{A}}_{l,\alpha}, \mathcal{E}^{\mathrm{A}}_{l,\alpha}, \mathcal{E}^{\mathrm{D}}_{l,\alpha}$ indicating the strategies at the αth step of the lth game, $\alpha \in \mathbb{N}$. Note that here we show the strategies with two subscripts representing the game and the step indices along the time axis. If $h^{\mathrm{A}} > h^{\mathrm{D}}$, only the attacker formulates its strategies after h^{D}th step. Similarly, if $h^{\mathrm{A}} < h^{\mathrm{D}}$, only the defender formulates its strategies after h^{A}th step. In the case of $h^{\mathrm{A}} = h^{\mathrm{D}}$, both players obtain their strategies until $(h^{\mathrm{A}} = h^{\mathrm{D}})$th step, denoted by $((\bar{\mathcal{E}}^{\mathrm{A}}_{l,1}, \mathcal{E}^{\mathrm{A}}_{l,1}, \mathcal{E}^{\mathrm{D}}_{l,1}), \ldots, (\bar{\mathcal{E}}^{\mathrm{A}}_{l,h^{\mathrm{A}}}, \mathcal{E}^{\mathrm{A}}_{l,h^{\mathrm{A}}}, \mathcal{E}^{\mathrm{D}}_{l,h^{\mathrm{A}}}))$.

However, since the game is played in a rolling horizon fashion, only $((\bar{\mathcal{E}}^{\mathrm{A}}_{l,1}, \mathcal{E}^{\mathrm{A}}_{l,1}, \mathcal{E}^{\mathrm{D}}_{l,1}), \ldots, (\bar{\mathcal{E}}^{\mathrm{A}}_{l,T}, \mathcal{E}^{\mathrm{A}}_{l,T}, \mathcal{E}^{\mathrm{D}}_{l,T}))$ is applied (recall that h^{A} and h^{D} are taken to be greater than or equal to T). Here the strategies applied can be written in single subscripts of time indices as $((\bar{\mathcal{E}}^{\mathrm{A}}_{(l-1)T}, \mathcal{E}^{\mathrm{A}}_{(l-1)T}, \mathcal{E}^{\mathrm{D}}_{(l-1)T}), \ldots, (\bar{\mathcal{E}}^{\mathrm{A}}_{lT-1}, \mathcal{E}^{\mathrm{A}}_{lT-1}, \mathcal{E}^{\mathrm{D}}_{lT-1})) = ((\bar{\mathcal{E}}^{\mathrm{A}}_{l,1}, \mathcal{E}^{\mathrm{A}}_{l,1}, \mathcal{E}^{\mathrm{D}}_{l,1}), \ldots, (\bar{\mathcal{E}}^{\mathrm{A}}_{l,T}, \mathcal{E}^{\mathrm{A}}_{l,T}, \mathcal{E}^{\mathrm{D}}_{l,T}))$. We assume that the values of h^{A} and h^{D} are known to both players. Note that this game is not necessarily zero-sum.

In what follows, we provide an example of a small scale to detail how the optimal edges can be obtained in our game setting. To this end, suppose that $h^{\mathrm{A}} = 3$ and $h^{\mathrm{D}} = 2$. The optimal strategies $((\bar{\mathcal{E}}^{\mathrm{A}*}_{l,1}, \mathcal{E}^{\mathrm{A}*}_{l,1}, \mathcal{E}^{\mathrm{D}*}_{l,1}), (\bar{\mathcal{E}}^{\mathrm{A}*}_{l,2}, \mathcal{E}^{\mathrm{A}*}_{l,2}, \mathcal{E}^{\mathrm{D}*}_{l,2}), (\bar{\mathcal{E}}^{\mathrm{A}*}_{l,3}, \mathcal{E}^{\mathrm{A}*}_{l,3}))$ of the players at the game with index l are obtained backward in time (from Step $\alpha = 3$ to Step $\alpha = 1$) and is given by:

- Step 3:

$$(\bar{\mathcal{E}}^{\mathrm{A}*}_{l,3}(\mathcal{E}^{\mathrm{D}}_{l,2}), \mathcal{E}^{\mathrm{A}*}_{l,3}(\mathcal{E}^{\mathrm{D}}_{l,2})) \in \arg \max_{(\bar{\mathcal{E}}^{\mathrm{A}}_{l,3}, \mathcal{E}^{\mathrm{A}}_{l,3})} U^{\mathrm{A}}_{l,3}(\mathcal{E}^{\mathrm{D}*}_{l,3}) \tag{6}$$

$$\text{where } \mathcal{E}^{\mathrm{D}*}_{l,3}(\bar{\mathcal{E}}^{\mathrm{A}}_{l,3}, \mathcal{E}^{\mathrm{A}}_{l,3}) \in \arg \max_{\mathcal{E}^{\mathrm{D}}_{l,3}} -U^{\mathrm{A}}_{l,3}, \tag{7}$$

- Step 2:

$$\mathcal{E}^{\mathrm{D}*}_{l,2}(\bar{\mathcal{E}}^{\mathrm{A}}_{l,2}, \mathcal{E}^{\mathrm{A}}_{l,2}) \in \arg \max_{\mathcal{E}^{\mathrm{D}}_{l,2}} U^{\mathrm{D}}_{l,2}, \tag{8}$$

$$(\bar{\mathcal{E}}^{\mathrm{A}*}_{l,2}(\mathcal{E}^{\mathrm{D}}_{l,1}), \mathcal{E}^{\mathrm{A}*}_{l,2}(\mathcal{E}^{\mathrm{D}}_{l,1})) \in \arg \max_{(\bar{\mathcal{E}}^{\mathrm{A}}_{l,2}, \mathcal{E}^{\mathrm{A}}_{l,2})} U^{\mathrm{A}}_{l,2}(\mathcal{E}^{\mathrm{D}*}_{l,2}), \tag{9}$$

- Step 1:

$$\mathcal{E}^{\mathrm{D}*}_{l,1}(\bar{\mathcal{E}}^{\mathrm{A}}_{l,1}, \mathcal{E}^{\mathrm{A}}_{l,1}) \in \arg \max_{\mathcal{E}^{\mathrm{D}}_{l,1}} U^{\mathrm{D}}_{l}(\bar{\mathcal{E}}^{\mathrm{A}\prime}_{l,2}, \mathcal{E}^{\mathrm{A}\prime}_{l,2}) \tag{10}$$

$$\text{where } (\bar{\mathcal{E}}^{\mathrm{A}\prime}_{l,2}(\mathcal{E}^{\mathrm{D}}_{l,1}), \mathcal{E}^{\mathrm{A}\prime}_{l,2}(\mathcal{E}^{\mathrm{D}}_{l,1})) \in \arg \max_{(\bar{\mathcal{E}}^{\mathrm{A}}_{l,2}, \mathcal{E}^{\mathrm{A}}_{l,2})} -U^{\mathrm{D}}_{l,2}(\mathcal{E}^{\mathrm{D}*}_{l,2}), \tag{11}$$

$$(\bar{\mathcal{E}}^{\mathrm{A}*}_{l,1}, \mathcal{E}^{\mathrm{A}*}_{l,1}) \in \arg \max_{(\bar{\mathcal{E}}^{\mathrm{A}}_{l,1}, \mathcal{E}^{\mathrm{A}}_{l,1})} U^{\mathrm{A}}_{l}(\mathcal{E}^{\mathrm{D}*}_{l,1}), \tag{12}$$

where $U^{\mathrm{A}}_{l,\alpha} := \sum_{k=(l-1)T+\alpha-1}^{(l-1)T+h^{\mathrm{A}}-1} -c(\mathcal{G}^{\mathrm{D}}_k)$ (resp., $U^{\mathrm{D}}_{l,\alpha} := \sum_{k=(l-1)T+\alpha-1}^{(l-1)T+h^{\mathrm{D}}-1} c(\mathcal{G}^{\mathrm{D}}_k)$) is defined as parts of U^{A}_l (resp., U^{D}_l) calculated from the αth step to the h^{A}th (resp., h^{D}th) step of the lth game.

Once again, these optimization problems are solved backward from the $\max\{h^{\mathrm{A}}, h^{\mathrm{D}}\} = 3$rd step of the lth game. Note that to find $(\bar{\mathcal{E}}^{\mathrm{A}*}_{l,1}, \mathcal{E}^{\mathrm{A}*}_{l,1})$ in (12), one needs to obtain $(\mathcal{E}^{\mathrm{D}*}_{l,1}(\bar{\mathcal{E}}^{\mathrm{A}}_{l,1}, \mathcal{E}^{\mathrm{A}}_{l,1}))$ in (10) beforehand. Likewise, to find $(\mathcal{E}^{\mathrm{D}*}_{l,1}(\bar{\mathcal{E}}^{\mathrm{A}}_{l,1}, \mathcal{E}^{\mathrm{A}}_{l,1}))$ in (10), one needs to obtain $(\bar{\mathcal{E}}^{\mathrm{A}*}_{l,2}(\mathcal{E}^{\mathrm{D}}_{l,1}), \mathcal{E}^{\mathrm{A}*}_{l,2}(\mathcal{E}^{\mathrm{D}}_{l,1}))$ in (9), and so on. Also, note that while $\mathcal{E}^{\mathrm{D}*}_{l,3}$ is not part of the defender's strategy, it is still needed for the attacker to obtain $(\bar{\mathcal{E}}^{\mathrm{A}*}_{l,3}, \mathcal{E}^{\mathrm{A}*}_{l,3})$ in (6). Therefore, outside the defender's ability characterized by its horizon length h^{D}, here we suppose that the attacker utilizes the strategy that emulates the defender's best response with a longer horizon, i.e., from part of utility functions $-U^{\mathrm{A}}_l$ (which is not equal to U^{D}_l due to the horizon inadequacy).

In the steps with index $\alpha \leq h^{\mathrm{D}}$, the defender assumes that the attacker's optimal edges, e.g., in (11), are based on the defender's utility function, which consists of $h^{\mathrm{D}} < h^{\mathrm{A}}$ steps only. Also, in this game the defender's optimal strategies, e.g., in (10), are based on the defender's perception of the attacker's optimal strategies, i.e., $(\bar{\mathcal{E}}^{\mathrm{A}\prime}_{l,2}, \mathcal{E}^{\mathrm{A}\prime}_{l,2})$, since the defender is not able to foresee the attacker's strategy beyond h^{D}. For the attacker, since it is able to compute the optimal strategy for the defender as well (due to longer h^{A}), the attacker's strategies in the steps with index $\alpha \leq h^{\mathrm{D}}$, e.g., (9) and (12), are based on the defender's optimal edges $\mathcal{E}^{\mathrm{D}*}_{l,\alpha}$.

In this setting, since the defender's strategy depends on the attacker's strategy as well, i.e., the defender can only recover edges attacked normally, it is possible that the defender cannot apply its strategy when the attacker changes its own strategy. In this case, the defender will apply the strategy only on the edges that can be recovered.

The decision-making process of the players in this example is illustrated in the game tree in Fig. 3, where the blue line indicates the *equilibrium path*. i.e., the strategy taken by the player following backward induction, if $h^{\mathrm{A}} = h^{\mathrm{D}} = 3$. The green line indicates the equilibrium path if $h^{\mathrm{A}} = h^{\mathrm{D}} = 2$ and the magenta line indicates the equilibrium path if $h^{\mathrm{A}} = 3, h^{\mathrm{D}} = 2$. In step 2, the attacker assumes that $\mathcal{E}^{\mathrm{D}*}_{l,2}$ comes from utility over $h^{\mathrm{A}} = 3$. The case where $h^{\mathrm{A}} < h^{\mathrm{D}}$ can be similarly described. These optimization problems are solved by the players at every game period T.

It is clear that with a longer T, the players play this game less often and apply their obtained strategies for more time steps. Note that with $T = \min\{h^{\mathrm{A}}, h^{\mathrm{D}}\}$, the player with a shorter horizon length does not change its strategies at all, thus effectively removing the rolling horizon aspect of the player. In this game, we will find the optimal strategies of the players by computing all possible combinations, since the choices of edges are finite.

From the optimization problems in (7)–(12) above, the player with a shorter horizon length $h_{\mathrm{short}} \in \{h^{\mathrm{A}}, h^{\mathrm{D}}\}$ examines at most $3^{|\mathcal{E}|}2^{|\mathcal{E}|}h_{\mathrm{short}}$ number of combinations for utility evaluations, since the player has to foresee the opponent's response as well. Note that the attacker has three possible actions on an edge: no attack, attack with normal signals, and attack with strong signals. On the other hand, the player with a longer horizon length $h_{\mathrm{long}} \in \{h^{\mathrm{A}}, h^{\mathrm{D}}\}$ examines at most $(3^{|\mathcal{E}|}2^{|\mathcal{E}|})(h_{\mathrm{long}} - h_{\mathrm{short}}) + (3^{|\mathcal{E}|} + 3^{|\mathcal{E}|}2^{|\mathcal{E}|})h_{\mathrm{long}}$ combinations.

In this section, we have explained the problem setting where it is assumed that the players may not have the same computational ability represented by the different values of horizon lengths h^{A} and h^{D}. Without the assumption of the horizon length discrepancy, the most related results are given in [13] where the play-

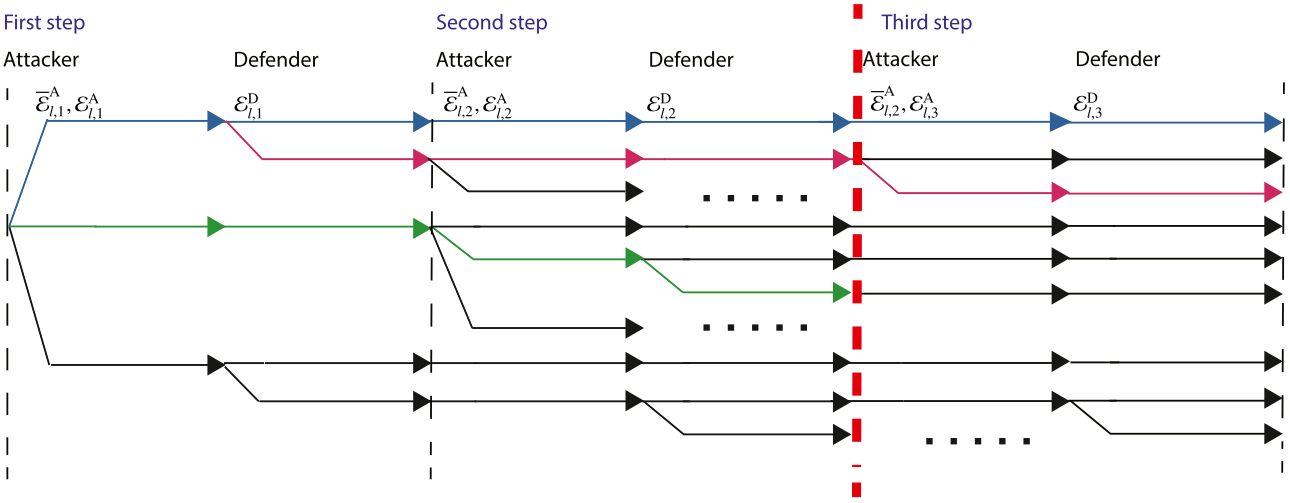

Fig. 3. Extensive-form game for $h^{\mathrm{A}} = 3$ and $h^{\mathrm{D}} = 2$. The vertical dashed lines denote the different steps of the game, whereas the dashed red line denotes boundary (min{2,3}) of different players' horizon lengths. The optimization beyond this boundary is done by only the player with a longer horizon (in this case the attacker).

ers have the same ability to compute their strategies, represented by $h^{\mathrm{A}} = h^{\mathrm{D}} = h$. There, we do not discuss the effect of the horizons on the players' performance; we instead focus more on the necessary and sufficient condition of agents clustering at infinite time, given the consensus dynamics. Other related papers include [4] which considers the one-shot attack-recovery games. This formulation is extended in [12] where the repeated attack-recovery games without rolling horizon approach in continuous time is considered. Specifically, the timings for launching attack/defense actions are also part of the decision variables. The problem setting where a game in continuous time is divided into several steps without rolling horizon approach is also discussed in [11].

4. Players' performance with non-uniform horizon lengths

The utility functions defined in (4) and (5) are considered for deriving the best strategies for the players. As explained in Section 2.1 above, the last several actions for the players may be discarded from the obtained strategies and replaced by a new set of actions calculated in the next game. As a consequence, the resulting values of the agent-group distribution at time k is given by $c(\mathcal{G}^{\mathrm{D}*}_k)$, with $\mathcal{G}^{\mathrm{D}*}_k = (\mathcal{V}, ((\mathcal{E} \setminus (\overline{\mathcal{E}}^{\mathrm{A}*}_k \cup \mathcal{E}^{\mathrm{A}*}_k)) \cup (\mathcal{E}^{\mathrm{D}*}_k \cap \mathcal{E}^{\mathrm{A}*}_k))$. We now characterize how the horizon lengths h^{A} and h^{D} affect the *applied utilities* $\hat{U}^{\mathrm{A}}_k := -c(\mathcal{G}^{\mathrm{D}*}_k)$ and $\hat{U}^{\mathrm{D}}_k := c(\mathcal{G}^{\mathrm{D}*}_k)$. These are elements of the utility functions U^{A}_l and U^{D}_l corresponding to the αth step, with $\alpha = k \bmod T+1$, of the game with index $l = \lfloor k/T \rfloor + 1$, where the obtained strategies $(\overline{\mathcal{E}}^{\mathrm{A}*}_{(l-1)T+\alpha-1}, \mathcal{E}^{\mathrm{A}*}_{(l-1)T+\alpha-1}, \mathcal{E}^{\mathrm{D}*}_{(l-1)T+\alpha-1}) = (\overline{\mathcal{E}}^{\mathrm{A}*}_{l,\alpha}, \mathcal{E}^{\mathrm{A}*}_{l,\alpha}, \mathcal{E}^{\mathrm{D}*}_{l,\alpha})$ are applied.

We first state a result implying that when the attacker has large enough energy supply characterized by ρ^{A}, the optimal strategies of both players do not depend on the horizon lengths. Specifically, if $\rho^{\mathrm{A}}/\overline{\beta}^{\mathrm{A}} \geq |\mathcal{E}|$, then the attacker will attack all edges of the underlying graph $\mathcal{G}$ at any time k, making the optimal strategies independent of h^{A} and h^{D}.

The results afterwards illustrate the performance of the players for different h^{A} and h^{D} in separate subsections assuming that

$$\rho^{\mathrm{A}}/\overline{\beta}^{\mathrm{A}} < |\mathcal{E}|. \tag{13}$$

4.1. Attacker's strategies with varying h^{A}

To show the change of the attacker's strategies, we consider certain scenarios where the defender's strategies are less reliant on the attacker's action. Specifically, by assuming certain values of ρ^{D} and β^{D}, it is possible that the defender's optimal strategies are always to recover all $\mathcal{E}^{\mathrm{A}}_k$.

In this subsection, we further assume that

$$\rho^{\mathrm{D}}/\beta^{\mathrm{D}} > |\mathcal{E}|, \tag{14}$$

implying that ρ^{D} is large enough so that there is always recovery from normally attacked edges at any step of the game. Furthermore, in Propositions 1 and 2 below, we suppose for simplicity of obtaining theoretical assertions that

$$\kappa^{\mathrm{A}} = \rho^{\mathrm{A}}, \tag{15}$$

i.e., the attacker has the same amount of supplied energy at any k, including at $k = 0$.

We first state a lemma describing a property of a class of graphs under attacks, where it is better for the attacker to attack as soon as it has the energy, rather than saving it to attack more edges later. For the statement of the following results, let $\bar{c}(\xi) := \min_{|\mathcal{E}'|=\xi} c((\mathcal{V}, \mathcal{E} \setminus \mathcal{E}'))$ denote the smallest value of agent-group distribution given the number of strongly attacked edges $\xi\,(< n-1)$.

Lemma 1. *Consider the case where the network topology $\mathcal{G}$ of the agents is given as the star graph and the attacker attacks ξ number of edges with strong signals. Suppose (13)–(14) hold. Then, for time interval $\hat{k}$, $\hat{k}\bar{c}(\xi) \leq \bar{c}(\hat{k}\xi)$ is always satisfied for any $\hat{k} \leq (n-1)/\xi$.*

Proof. In the star graph $\mathcal{G}$, ξ number of strongly attacked edges results in ξ number of isolated agents and a group of $(n-\xi)$ number of agents forming a star graph. Thus, we have $\bar{c}(\xi) = (n-\xi)^2 + \xi - n^2$ and hence $\bar{c}(\hat{k}\xi) = (n-\hat{k}\xi)^2 + \hat{k}\xi - n^2$ so long as $\hat{k}\xi \leq n-1$. It then follows that the sum of agent-group distribution over $\hat{k}$ interval becomes $\hat{k}\bar{c}(\xi) = \hat{k}(n-\xi)^2 + \hat{k}\xi - \hat{k}n^2$. It is straightforward to show that $\hat{k}(n-\xi)^2 - \hat{k}n^2 \leq (n-\hat{k}\xi)^2 - n^2$ for any $\hat{k} \leq (n-1)/\xi$. □

In Lemma 1, we state that in the star graph attacking a few edges every time results in a more negative agent-group distribution compared to saving energy and only attacking later. For example, attacking one edge for $k = 1, 2$ results in a more negative $c(\mathcal{G}^{\mathrm{D}}_1) + c(\mathcal{G}^{\mathrm{D}}_2)$ over $\hat{k} = 2$ interval than attacking two edges only for one time $k = 2$; $(n-1)^2 + (n-1)^2 \leq n^2 + (n-2)^2$ from (3) is always satisfied (note that the value of agent-group distribution is zero if there is no attack).

Proposition 1. *Consider the case where the network topology $\mathcal{G}$ of the agents is given by any tree graph. Suppose that (13)–(15) hold. Then, the value of $\sum_{k=0}^{\bar{k}} \hat{U}_k^{\mathrm{A}}$ does not depend on h^{A} or T, for any time $\bar{k}$.*

Proof. Since after the attack of $|\bar{\mathcal{E}}_k^{\mathrm{A}}|$ edges there is still a group of agents consisting of at most $(n-|\bar{\mathcal{E}}_k^{\mathrm{A}}|)$ agents forming a star graph, here the star graph gives the least value of agent-group distribution among the graphs with n nodes with edge connectivity 1 (tree graphs). Therefore, proving for the star graph is sufficient to show the result for the tree graphs.

Since the immediate attack gives the more negative agent-group distribution from Lemma 1, it then follows that if $\kappa^{\mathrm{A}} = \rho^{\mathrm{A}}$, it will also give the maximum $\sum_{k=0}^{\bar{k}} \hat{U}_k^{\mathrm{A}}$ over any $\bar{k}$. Note that, if $\kappa^{\mathrm{A}} > \rho^{\mathrm{A}}$, i.e., (15) is not satisfied, then the attacker may have different ability especially at $k=0$, which makes the immediate attack more wasteful and no longer optimal in a shorter horizon situation. □

We continue by stating a result on the complete graph $\mathcal{G}$, where in a low energy situation characterized by small $\rho^{\mathrm{A}}/\bar{\beta}^{\mathrm{A}}$, the attacker with longer h^{A} always has better utility.

Proposition 2. *Consider the complete graph $\mathcal{G}$. If (13)–(15) and $\rho^{\mathrm{A}}/\bar{\beta}^{\mathrm{A}} < (n-2)/T$ are satisfied, then $0 = \sum_{k=0}^{\bar{k}} \hat{U}_k^{\mathrm{A}}(h^{\mathrm{A}} = T) \leq \sum_{k=0}^{\bar{k}} \hat{U}_k^{\mathrm{A}}(h^{\mathrm{A}} > T)$ for any $\bar{k}$.*

Proof. Note that the complete graph has the edge connectivity $n-1$. Since it is assumed that the attacker always spends all of its energy at the last step of the game, there is at most $\bar{\beta}^{\mathrm{A}}$ amount of energy at the beginning of each game from the leftover of the previous games. With $\rho^{\mathrm{A}} T < (n-2)\bar{\beta}^{\mathrm{A}}$, if $h^{\mathrm{A}} = T$, then the attacker will spend all of its energy at the last step of the game without disconnecting any agent, implying that $U_l^{\mathrm{A}} = 0$ for any l and hence $\hat{U}_k^{\mathrm{A}} = 0$ for any k. □

In Proposition 3 below, we state that the attacker with a shorter h^{A} in any $\mathcal{G}$ may perform better if we measure the applied utility over a shorter interval.

Proposition 3. *Suppose that (13) and (14) are satisfied. In any $\mathcal{G}$, it follows that $\sum_{k=0}^{\bar{k}} \hat{U}_k^{\mathrm{A}}(h^{\mathrm{A}} = 1) \geq \sum_{k=0}^{\bar{k}} \hat{U}_k^{\mathrm{A}}(h^{\mathrm{A}} > 1)$ for any time $\bar{k} < \lfloor \kappa^{\mathrm{A}}/(|\mathcal{E}|\bar{\beta}^{\mathrm{A}} - \rho^{\mathrm{A}}) \rfloor$.*

Proof. In the case of $h^{\mathrm{A}} = 1$, at time $k=0$ the attacker will spend all its energy, which is dictated by κ^{A}. In this case, if $\kappa^{\mathrm{A}} > |\mathcal{E}|\bar{\beta}^{\mathrm{A}}$, then the attacker will attack all edges to maximize U_l^{A}. Considering the recharge rate ρ^{A} that changes the attacker's available energy in each time k, the attacker with $h^{\mathrm{A}} = 1$ will attack all edges with strong signals as long as k satisfies $k < \frac{\kappa^{\mathrm{A}} + k\rho^{\mathrm{A}}}{|\mathcal{E}|\bar{\beta}^{\mathrm{A}}}$. It then follows that, since attacking all edges always gives maximum applied utility in a single time step, with $h^{\mathrm{A}} = 1$ the attacker will obtain maximum possible applied utility $\hat{U}_k^{\mathrm{A}}$ for time $k < \frac{\kappa^{\mathrm{A}} + k\rho^{\mathrm{A}}}{|\mathcal{E}|\bar{\beta}^{\mathrm{A}}}$. □

4.2. Defender's strategies with varying h^{D}

In this section, we discuss the characterization of $\hat{U}_k^{\mathrm{D}}$ of the defender given different values of h^{D}. We first state a lemma describing a property of an attacked empty graph $(\mathcal{V}, \emptyset)$, where it is better for the defender to save its energy and use it later to recover more edges. For the statement of the following results, let $c'(\theta) := \max_{|\mathcal{E}'|=\theta} c((\mathcal{V}, \mathcal{E}'))$ denote the largest value of agent-group distribution given the number of recovered edges θ. As a consequence, $\sum_{k=0}^{\hat{k}} c'(\theta) = \hat{k}c'(\theta)$ indicates the energy consumption when the number of recovered edges is θ for $\hat{k}$ steps.

Lemma 2. *Assume that the attacker attacks all edges $\mathcal{E}$ with normal signals at all time. Let θ be the number of recovered edges. If (13) is satisfied, then*

$$\hat{k}c'(\theta) \leq (\hat{k}-1)c'(0) + c'(\hat{k}\theta) \tag{16}$$

for any time interval $\hat{k} \leq (n-1)/\theta$ for any $\theta = 1, \ldots, n-1$.

Proof. We begin by discussing the right-hand side of (16). Recall from (3) that $c'(0) = c((\mathcal{V}, \emptyset)) = n - n^2$. Note that, in the last time step of $\hat{k} \leq (n-1)/\theta$ interval, the defender cannot recover more than $(n-1)$ edges given no previous recovery for $\hat{k}-1$ interval. Thus, at the end of the interval, (3) becomes $c'(k\theta) = (\hat{k}\theta + 1)^2 + (n - \hat{k}\theta - 1) - n^2$.

On the other hand, if the defender recovers θ number of edges, then we have $c'(\theta) = (\theta+1)^2 + (n-\theta-1) - n^2$. It then follows that $\hat{k}c'(\theta) = \hat{k}[(\theta+1)^2 + (n-\theta-1) - n^2] \leq (\hat{k}-1)c'(0) + c'(\hat{k}\theta) = (\hat{k}-1)n + (\hat{k}\theta+1)^2 + (n - \hat{k}\theta - 1) - \hat{k}n^2$ for any time interval $\hat{k} \leq (n-1)/\theta$. □

From (5), we note that the defender prefers strategies that result in larger value of $c(\mathcal{G}_k^{\mathrm{D}})$ over time. Thus, by Lemma 2, we see that recovering later is better for the defender, which is different from Lemma 1 for the attacker where attacking immediately is better.

We now continue by assuming certain values of the attacker's energy parameters so that its strategies do not change regardless of the defender's response. Specifically, we now assume that

$$\kappa^{\mathrm{A}} = \rho^{\mathrm{A}} = \beta^{\mathrm{A}}|\mathcal{E}|, \quad \bar{\beta}^{\mathrm{A}}/\beta^{\mathrm{A}} > h^{\mathrm{A}}|\mathcal{E}| \tag{17}$$

are satisfied, i.e., attacking with strong signals takes much energy so that it is not affordable for the attacker to take such actions at any time. Note that with $\rho^{\mathrm{A}} = \beta^{\mathrm{A}}|\mathcal{E}|$, the attacker will be able to attack all edges normally at all time; furthermore, with $\bar{\beta}^{\mathrm{A}}/\beta^{\mathrm{A}} > h^{\mathrm{A}}|\mathcal{E}|$ the attacker will never have enough energy to attack any edge with strong signals at any step of the game. Therefore, any attacked edge at any time can be recovered.

In Proposition 4, similar to Proposition 3 above, we now state that the defender with a shorter h^{D} may perform better if we measure the applied utility over a shorter interval. Note that this result does not depend on the topology of the underlying graph $\mathcal{G}$, similar to the one in Proposition 3 above.

Proposition 4. *Suppose that $\rho^{\mathrm{D}}/\beta^{\mathrm{D}} < n-1$ and (17) are satisfied. Then $\sum_{k=0}^{\bar{k}} U_l^{\mathrm{D}}(h^{\mathrm{D}} = 1) \geq \sum_{k=0}^{\bar{k}} U_l^{\mathrm{D}}(h^{\mathrm{D}} > 1)$ is satisfied, with $\bar{k} < \lfloor \frac{\kappa^{\mathrm{D}}}{(n-1)\beta^{\mathrm{D}} - \rho^{\mathrm{D}}} \rfloor$.*

Proof. Since $\bar{\beta}^{\mathrm{A}}/\beta^{\mathrm{A}}$ is large enough to prevent attacking with strong signals, all attacks in any k are done with normal jamming signals. Since $\rho^{\mathrm{A}}/\beta^{\mathrm{A}} = |\mathcal{E}|$, the attacker is able to attack all edges $\mathcal{E}$ at all k, which is optimal.

Similar to the proof in Proposition 3 above, since the defender recovers all of the attacked edges with $h^{\mathrm{D}} = 1$, at $k=0$ it will obtain maximum applied utility. The assumption $\rho^{\mathrm{D}}/\beta^{\mathrm{D}} < n-1$ means that the defender cannot recover more than $(n-1)$ number of edges at every time k, which results in maximum $c(\mathcal{G}_k^{\mathrm{D}})$ in (3). The defender then will recover all edges until time $\lfloor \frac{\kappa^{\mathrm{D}}}{(n-1)\beta^{\mathrm{D}} - \rho^{\mathrm{D}}} \rfloor$. □

While we do not obtain the general condition that ensures a higher utility for longer h^{A} (resp., longer h^{D}), in Section 6 we will show in a numerical simulation that with longer horizons the attacker (resp., the defender) generally obtains more applied utility over longer time.

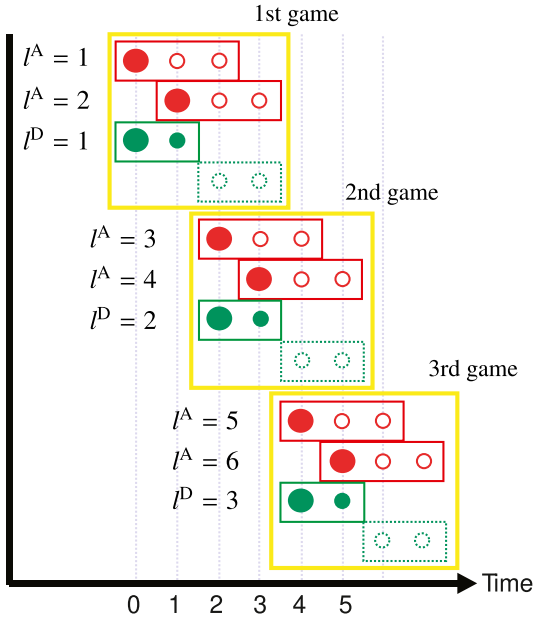

Fig. 4. Sequence of games with decision-making indices l^A and l^D: the attacker's horizon (red) and the defender's horizon (green) with non-uniform game periods. The horizon lengths are $h^A = 3$ and $h^D = 2$, whereas the game periods are $T^A = 1$ and $T^D = 2$.

5. Game structure and players' performance with non-uniform game periods

5.1. Game structure with non-uniform game periods

In this section, we extend the problem formulation by generalizing the game period T into T^A and T^D for the attacker and the defender, respectively. These periods T^A and T^D are known by both players for simplicity of the analysis. To ensure that both players are able to obtain their own strategies at any k, we set $T^A \leq h^A$ and $T^D \leq h^D$. The game with non-uniform game periods is illustrated in Fig. 4. Each of the yellow rectangle indicates a game consisting of the set of *decision-making processes*, which follows a certain pattern. A game is played, i.e., both players simultaneously update their strategies, every lowest common multiple of T^A and T^D denoted as $\mathrm{lcm}(T^A, T^D)$; in Fig. 4, the game is played every 2 time steps. With this formulation, it is expected that the players have better performance with shorter T^A and T^D since they can adapt to the changes faster.

From Fig. 4, we see that the players may not formulate their strategies at the same time. For example, at time $k = 1$, only the attacker updates its strategies, whereas the defender does not due to the longer T^D. Since T^A and T^D are known by both players, at $k = 1$ the attacker decides its strategy considering the defender's strategy that is obtained before at $k = 0$. Furthermore, since $h^A = 3$ and $\mathcal{E}^D_{1,2}$ has been determined, here the attacker at $k = 1$ with the ability to compute for three time steps ahead predicts and hence already covers the defender's second decision-making process. This attacker's prediction of the defender's next actions is represented by the green rectangle with dashed lines in Fig. 4.

Since it is clear that the non-uniform game periods make the players decide their strategies at different times, we specify different decision-making indices l^A and l^D which occur at times $(l^A - 1)T^A$ and $(l^D - 1)T^D$ for the attacker and the defender, respectively. As a result, the attacker (resp., the defender) does not update its strategy if $k \pmod{T^A} \neq 0$ (resp., $k \pmod{T^D} \neq 0$). The utility functions of the l^Ath and l^Dth decision-making processes consisting of α^A and α^D steps, respectively, are given by

$$U^A_{l^A} := \sum_{k=(l^A-1)T^A}^{(l^A-1)T^A+h^A-1} -c(\mathcal{G}^D_k) = \sum_{\alpha^A=1}^{h^A} -c(\mathcal{G}^D_{l^A,\alpha^A}), \tag{18}$$

$$U^D_{l^D} := \sum_{k=(l^D-1)T^D}^{(l^D-1)T^D+h^D-1} c(\mathcal{G}^D_k) = \sum_{\alpha^D=1}^{h^D} c(\mathcal{G}^D_{l^D,\alpha^D}), \tag{19}$$

similar to (4) and (5) above. Note that different values of these indices for the players may refer to the same time step; e.g., in Fig. 4, both $l^A = 2$, $\alpha^A = 1$ and $l^D = 1$, $\alpha^D = 2$ correspond to $k = 1$.

The optimal strategy of the attacker at time $k = 1$ corresponding to $l^A = 2$, i.e., $((\overline{\mathcal{E}}^{A*}_{2,1}, \mathcal{E}^{A*}_{2,1}), (\overline{\mathcal{E}}^{A*}_{2,2}, \mathcal{E}^{A*}_{2,2}), (\overline{\mathcal{E}}^{A*}_{2,3}, \mathcal{E}^{A*}_{2,3}))$ in the case shown in Fig. 4 (noting that $k \pmod{T^A} = 0$ and $k \pmod{T^D} \neq 0$ for $k = 1$), is obtained backward in time and are given by:

- Step 3 ($k = 3$, $l^D = 2$):

$$(\overline{\mathcal{E}}^{A*}_{2,3}(\mathcal{E}^D_{2,2}), \mathcal{E}^{A*}_{2,3}(\mathcal{E}^D_{2,2})) \in \arg\max_{(\overline{\mathcal{E}}^A_{2,3}, \mathcal{E}^A_{2,3})} U^A_{2,3}(\mathcal{E}^{D\prime}_{2,2}) \tag{20}$$

  where $\mathcal{E}^{D\prime}_{2,2}(\overline{\mathcal{E}}^A_{2,3}, \mathcal{E}^A_{2,3}) \in \arg\max_{\mathcal{E}^D_{2,2}} -U^A_{2,3}$,

- Step 2 ($k = 2$, $l^D = 2$):

$$(\overline{\mathcal{E}}^{A*}_{2,2}(\mathcal{E}^D_{2,1}), \mathcal{E}^{A*}_{2,2}(\mathcal{E}^D_{2,1})) \in \arg\max_{(\overline{\mathcal{E}}^A_{2,2}, \mathcal{E}^A_{2,2})} U^A_{2,2}(\mathcal{E}^{D\prime}_{2,1}) \tag{21}$$

  where $\mathcal{E}^{D\prime}_{2,1}(\overline{\mathcal{E}}^A_{2,2}, \mathcal{E}^A_{2,2}) \in \arg\max_{\mathcal{E}^D_{2,1}} -U^A_{2,2}(\overline{\mathcal{E}}^{A*}_{2,3}, \mathcal{E}^{A*}_{2,3})$,

- Step 1 ($k = 1$, $l^D = 1$):

$$(\overline{\mathcal{E}}^{A*}_{2,1}, \mathcal{E}^{A*}_{2,1}) \in \arg\max_{(\overline{\mathcal{E}}^A_{2,1}, \mathcal{E}^A_{2,1})} U^A_2(\mathcal{E}^D_1). \tag{22}$$

Since the attacker cannot compute more than $h^A = 3$ time steps ahead, in (20) and (21) above the attacker will use its own utility function $U^A_{l^A}$ to estimate the defender's optimal edges denoted by $\mathcal{E}^{D\prime}_{2,\alpha}$, i.e., at $l^D = 2$. Since $1 \pmod{T^D} \neq 0$, the defender does not make a new decision and thus will apply the strategy obtained in the previous time instead. Therefore, it is possible for the player with shorter game period (in this case, the attacker) to benefit by changing its strategies; for example, in the case explained above, the attacker may benefit by changing $\mathcal{E}^A_1$ to avoid the recovery by the defender $\mathcal{E}^D_1$, which has been set and cannot be changed.

The optimization problems explained above vary slightly at each time due to different T^A and T^D. For example, the optimization problems (20)–(22) are solved at times $k = i(\mathrm{lcm}(T^A, T^D)) + 1$, $i \in \mathbb{N}_0$.

5.2. Attacker's strategies with varying T^A

In this section, we also explore the performance of the attacker represented by $\hat{U}^A_k$ for the non-uniform game periods, similar to the one in Section 4 above. We first state that under some condition, the values of T^A and T^D do not affect the optimal strategies of the players.

Specifically, we notice that if $\rho^A/\overline{\beta}^A \geq |\mathcal{E}|$, the attacker attacks all of the edges of $\mathcal{G}$ at any time k, making the optimal strategies, and therefore the applied utilities $\hat{U}^A_k$ and $\hat{U}^D_k$, independent of the values of T^A and T^D.

We continue by discussing the strategies of the players given that $\rho^A/\overline{\beta}^A < |\mathcal{E}|$, i.e., (13), is satisfied. In Corollaries 1–3 and Proposition 5 below, we also suppose that (14) and (15) are satisfied, for the same reason as in Section 4 above. The result in

Corollary 1 below for the tree graph $\mathcal{G}$ is also similar to the one in Section 4, since the optimal strategies for both players do not rely on T^{A}.

Corollary 1. *Consider the tree graph $\mathcal{G}$. If (13)–(15) are satisfied, then $\sum_{k=0}^{\bar{k}} \hat{U}_k^{\mathrm{A}}$ does not depend on h^{A} or T^{A}, for any time $\bar{k}$.*

Proof. The proof is similar to the proof of Proposition 1. □

We then state the attacker's optimal strategies for $T^{\mathrm{A}} = 1$ under certain situations for the case of the complete graph $\mathcal{G}$, where the attacker with low recharge rate ρ^{A} will not be able to attack any edge at earlier times.

Proposition 5. *Consider the complete graph $\mathcal{G}$. If (13)–(15), $\rho^{\mathrm{A}}/\overline{\beta}^{\mathrm{A}} < n-1$, and $T^{\mathrm{A}} = 1$ hold, then the attacker does not attack any edge for $k < \lfloor \frac{(h^{\mathrm{A}}-1)((n-1)-\rho^{\mathrm{A}}/\overline{\beta}^{\mathrm{A}})\rho^{\mathrm{A}}}{\overline{\beta}^{\mathrm{A}}} \rfloor$.*

Proof. Since $\kappa^{\mathrm{A}} = \rho^{\mathrm{A}} < (n-1)\overline{\beta}^{\mathrm{A}}$, the attacker keeps spending all of its energy and hence it cannot disconnect the graph by attacking with strong signals at any k. This implies that in the complete graph $\mathcal{G}$ the attacker will not attack unless it has enough energy to attack $n-1$ edges at later steps of the decision-making process. Furthermore, to implement the attack strategies, the attacker needs to have enough energy to attack at least $(n-1)h^{\mathrm{A}}$ number of edges (recall that given the same utility, the attacker is assumed to attack less edges at the earlier steps).

We are then looking for the condition that prevents the attacker from attacking at the earliest step (since $T^{\mathrm{A}} = 1$, the only applied strategies are the ones in the first step). With the ability to attack $\lfloor \rho^{\mathrm{A}}/\overline{\beta}^{\mathrm{A}} \rfloor$ number of edges every k, the attacker will have $(h^{\mathrm{A}}-1)\rho^{\mathrm{A}}/\overline{\beta}^{\mathrm{A}}$ more energy at the end of each game, given no previous attacks. It follows that there is no attack before time $\lfloor ((h^{\mathrm{A}}-1)(n-1) - (h^{\mathrm{A}}-1)\rho^{\mathrm{A}}/\overline{\beta}^{\mathrm{A}})/(\rho^{\mathrm{A}}/\overline{\beta}^{\mathrm{A}}) \rfloor$. □

From Proposition 5, we are able to characterize the attacker's performance measured by $\sum \hat{U}_k^{\mathrm{A}}$ for different T^{A} values in Corollary 2 below.

Corollary 2. *Consider the complete graph $\mathcal{G}$. If (13)–(15) and $\rho^{\mathrm{A}}/\overline{\beta}^{\mathrm{A}} < n-1$ hold, then the attacker's applied utilities satisfy $\sum_{k=0}^{\bar{k}} \hat{U}_k^{\mathrm{A}}(T^{\mathrm{A}}=1) < \sum_{k=0}^{\bar{k}} \hat{U}_k^{\mathrm{A}}(T^{\mathrm{A}}>1)$, with $\bar{k} < \lfloor (h^{\mathrm{A}}-1)((n-1) - \rho^{\mathrm{A}}/\overline{\beta}^{\mathrm{A}})(\overline{\beta}^{\mathrm{A}}/\rho^{\mathrm{A}}) \rfloor$.*

Proof. The result is a direct consequence of Proposition 5. □

From Proposition 2, we are also able to state that having a shorter T^{A} may help in the situation of low energy characterized by low $\rho^{\mathrm{A}}/\overline{\beta}^{\mathrm{A}}$.

Corollary 3. *Consider the complete graph $\mathcal{G}$. If (13)–(15) and $\rho^{\mathrm{A}}/\overline{\beta}^{\mathrm{A}} < (n-2)/h^{\mathrm{A}}$ are satisfied, then $\sum_{k=0}^{\bar{k}} \hat{U}_k^{\mathrm{A}}(T^{\mathrm{A}} < h^{\mathrm{A}}) \geq \sum_{k=0}^{\bar{k}} \hat{U}_k^{\mathrm{A}}(T^{\mathrm{A}} = h^{\mathrm{A}})$ for any $\bar{k}$.*

Proof. The result is a direct consequence of Proposition 2. □

5.3. Defender's strategies with varying T^{D}

In this section, we discuss the optimal strategies of the defender for different T^{D} values. In Proposition 6 and Corollary 4 below, we suppose that, again for simplicity, (17) and $\kappa^{\mathrm{D}} = \rho^{\mathrm{D}}$ are satisfied.

Proposition 6. *Suppose that (17) and $\kappa^{\mathrm{D}} = \rho^{\mathrm{D}}$ are satisfied. The defender with $T^{\mathrm{D}} = 1$ does not make any recovery for $k < \lfloor \frac{(h^{\mathrm{D}}-1)(n-1-\rho^{\mathrm{D}}/\beta^{\mathrm{D}})\beta^{\mathrm{D}}}{\rho^{\mathrm{D}}} \rfloor$.*

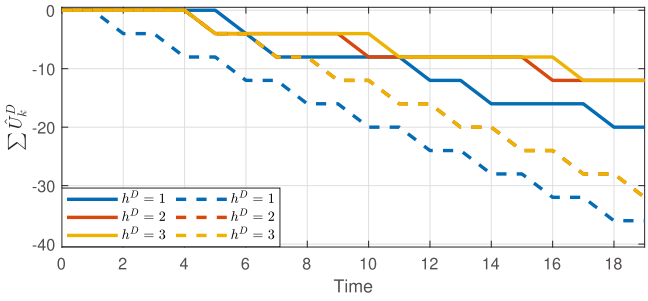

Fig. 5. Evolution of $\sum \hat{U}_k^{\mathrm{D}}$ for the path graph (solid lines) and the complete graph (dashed lines) with $h^{\mathrm{A}} = 1$; the results for complete graph with $h^{\mathrm{D}} = 2$ and $h^{\mathrm{D}} = 3$ are identical.

Proof. Since $\rho^{\mathrm{A}}/\beta^{\mathrm{A}} = |\mathcal{E}|$ and $\overline{\beta}^{\mathrm{A}}/\beta^{\mathrm{A}} > h^{\mathrm{A}}|\mathcal{E}|$ are satisfied by (17), the attacker cannot strongly attack any edge at any k and instead its optimal strategy is to attack $\mathcal{E}$ with normal jamming signals so that $\mathcal{G}_k^{\mathrm{A}}$ is an empty graph.

In this case, it follows from Lemma 2 that the defender will not recover any edge at the first step. Since by (3) the defender does not receive any additional utility by recovering more than $(n-1)$ edges, it then follows that to obtain the maximum utility of (19) in a single decision-making process, the defender has to recover $(n-1)h^{\mathrm{D}}$ number of edges in total ($(n-1)h^{\mathrm{D}}$ number of edges except for the $T^{\mathrm{D}}(=1)$ step(s)).

We continue by looking for the condition that prevents the defender from recovering at the first step. With the ability to recover $\lfloor \rho^{\mathrm{D}}/\beta^{\mathrm{D}} \rfloor$ number of edges every k, the defender projects that it will have $(h^{\mathrm{D}}-1)\rho^{\mathrm{D}}/\beta^{\mathrm{D}}$ more energy at the end of each decision-making process, given no previous recoveries. It then follows that the defender does not make any recovery before $\lfloor ((h^{\mathrm{D}}-1)(n-1) - (h^{\mathrm{D}}-1)\rho^{\mathrm{D}}/\beta^{\mathrm{D}})/(\rho^{\mathrm{D}}/\beta^{\mathrm{D}}) \rfloor$. □

From Proposition 6, we are able to characterize the defender's performance in Corollary 4 below.

Corollary 4. *Suppose that (17) and $\kappa^{\mathrm{D}} = \rho^{\mathrm{D}}$ are satisfied. Then the defender's observed utilities satisfy $\sum_{k=0}^{\bar{k}} \hat{U}_k^{\mathrm{D}}(T^{\mathrm{D}}=1) < \sum_{k=0}^{\bar{k}} \hat{U}_k^{\mathrm{D}}(T^{\mathrm{D}}>1)$ for $\bar{k} < \lfloor \frac{(h^{\mathrm{D}}-1)(n-1-\rho^{\mathrm{D}}/\beta^{\mathrm{D}})\beta^{\mathrm{D}}}{\rho^{\mathrm{D}}} \rfloor$.*

Proof. The result is a direct consequence of Proposition 6. □

These theoretical results on the case with varying T^{A} and T^{D} are specific to some values of parameters and class of graphs. We will see the performance of the players on more general graphs and parameters in Section 6 below.

6. Numerical examples

In this section, we provide some numerical examples to illustrate the difference of players' performance for the cases with non-uniform horizon lengths and game periods.

6.1. Non-uniform players' horizon lengths h^{A} and h^{D}

Here we discuss the players' strategies when they have non-uniform horizon lengths. It is expected that players will get better utility with longer horizon lengths, especially in the long term. From Figs. 5 and 6 plotting $\sum \hat{U}_k^{\mathrm{A}}$ and $\sum \hat{U}_k^{\mathrm{D}}$ over time with three different values of h^{A} and h^{D}, we see that it is generally the case in this simulation. In Fig. 5 for varying h^{D}, the parameters used are $n = 3$, $\rho^{\mathrm{A}}/\beta^{\mathrm{A}} = 3.1$, $\overline{\beta}^{\mathrm{A}}/\beta^{\mathrm{A}} = 10$, and $\rho^{\mathrm{D}}/\beta^{\mathrm{D}} = 1.5$. In this figure, we see that both in the path graph and the complete graph $\mathcal{G}$, the defender with $h^{\mathrm{D}} = 2$ and $h^{\mathrm{D}} = 3$ generally obtains more $\sum \hat{U}_k^{\mathrm{D}}$ than the one with $h^{\mathrm{D}} = 1$. The difference between $h^{\mathrm{D}} = 2$

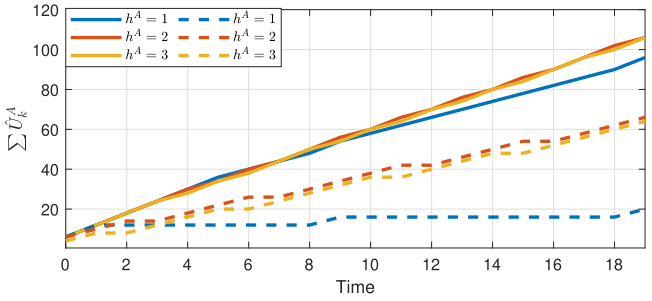

Fig. 6. Evolution of $\sum \hat{U}_k^{\mathrm{A}}$ with $h^{\mathrm{D}} = 1$ for the path graph (solid lines) and the complete graph (dashed lines).

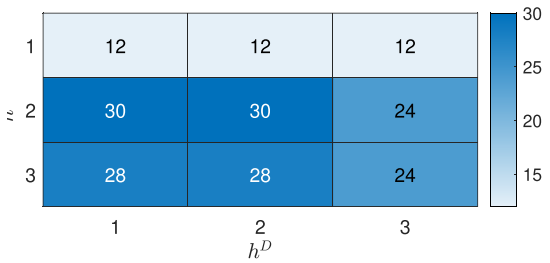

Fig. 7. $\sum_{k=0}^{20} \hat{U}_k^{\mathrm{A}}$ for different values of h^{A} and h^{D} for the complete graph.

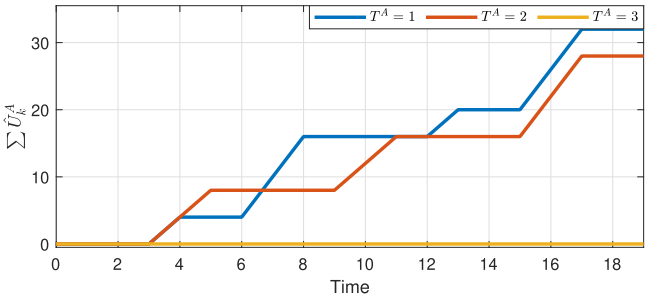

Fig. 8. Evolution of $\sum \hat{U}_k^{\mathrm{A}}$ for the complete graph with varying T^{A} and fixed $h^{\mathrm{A}} = 3$.

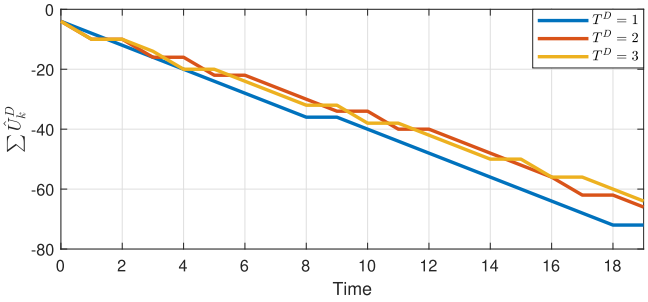

Fig. 9. Evolution of $\sum \hat{U}_k^{\mathrm{D}}$ for the path graph with varying T^{D} and fixed $h^{\mathrm{D}} = 3$.

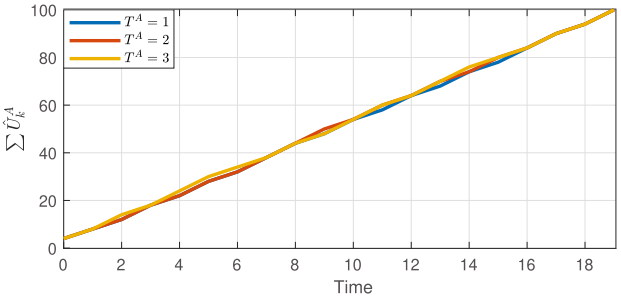

Fig. 10. Evolution of $\sum \hat{U}_k^{\mathrm{A}}$ for the path graph with varying T^{A} and fixed $h^{\mathrm{A}} = 3$.

and $h^{\mathrm{D}} = 3$ is not very significant in this simulation; it may be more notable in the case of more complex systems with more agents.

However, if we consider the performance of the players over a certain interval, it is possible that with a shorter horizon length the player can obtain more applied utility. We illustrate this phenomenon in the case of the attacker's applied utilities $\hat{U}_k^{\mathrm{A}}$ over time in Fig. 6. We now use parameters $\kappa^{\mathrm{A}} = 10.5$, $\overline{\beta}^{\mathrm{A}} = 2$, $\rho^{\mathrm{A}} = 2.5$, $h^{\mathrm{D}} = 3$, and $\rho^{\mathrm{D}}/\beta^{\mathrm{D}} = 5$, so that the condition $\rho^{\mathrm{D}}/\beta^{\mathrm{D}} > |\mathcal{E}|$ in Proposition 3 is satisfied. Note that $\kappa^{\mathrm{A}} > \rho^{\mathrm{A}}$ here, which does not satisfy the assumption of some of the results in Section 4. We see from Fig. 6 that the attacker with $h^{\mathrm{A}} = T = 1$ obtains a higher applied utility $\hat{U}_k^{\mathrm{A}}$ in the complete graph $\mathcal{G}$ until $k = 2$ as stated in Proposition 3, with $\overline{k} < 3$.

It is interesting to note that the complexity of the graph $\mathcal{G}$ also influences the effectiveness of having a longer horizon. Especially, with more connected $\mathcal{G}$, having a longer horizon may be even more beneficial, i.e., resulting in an even higher difference of total applied utility, compared to the case with less connected $\mathcal{G}$. For example, in Fig. 6, the difference of $\sum \hat{U}_k^{\mathrm{A}}$ in the complete graph is more apparent than in the path graph. The reason is that in the complete graph, since the attacker may attack some unnecessary edges in a short h^{A} case, e.g., attack all edges in $\mathcal{G}$, which makes the attacker have no energy in later time steps.

Fig. 7 shows $\sum_{k=0}^{20} \hat{U}_k^{\mathrm{A}}$ for several combinations of h^{A} and h^{D} with slightly different parameters, where similar to Fig. 6, the attacker obtains higher applied utility with $h^{\mathrm{A}} = 2$ and $h^{\mathrm{A}} = 3$, compared to that of $h^{\mathrm{A}} = 1$. Similarly, the defender also obtains more applied utility with a longer h^{D} (recall that $\hat{U}_k^{\mathrm{A}} = -\hat{U}_k^{\mathrm{D}}$).

6.2. Non-uniform players' game period T^{A} and T^{D}

In the situation where players have non-uniform game periods, we expect that players will get better utility over time with a shorter game period, since they can use their energy more efficiently. However, from Figs. 8–10, we see that the effectiveness of having a shorter game period depends on the underlying graph structure as well. In Fig. 8, the attacker obtains more applied utility in shorter game periods $T^{\mathrm{A}} = 1$ and $T^{\mathrm{A}} = 2$. On the other hand, in Fig. 10 the attacker in the path graph $\mathcal{G}$ obtains very similar utilities across different values of T^{A} and in Fig. 9 the defender with a longer T^{D} has slightly more applied utility over time.

For the simulation in Fig. 8, we consider the complete graph, with low recharge rate ρ^{A} for the attacker; specifically, we set $n = 3$, $h^{\mathrm{A}} = 3$, $\rho^{\mathrm{A}} = 0.9$, $\overline{\beta}^{\mathrm{A}} = 2$, and $\rho^{\mathrm{D}}/\beta^{\mathrm{D}} > 3$. Note that here, the attacker cannot attack strongly without saving energy. From Fig. 8, we see that in a low energy condition, having a long game period $T^{\mathrm{A}} = 3$ results in a lower utility over time. This is in line with Corollary 3 above, where having the maximum T^{A}, i.e., $T^{\mathrm{A}} = h^{\mathrm{A}}$, does not yield any additional applied utility, since the attacker becomes wasteful.

On the other hand, in Figs. 9 and 10 for the path graph, we observe that having higher update frequencies, i.e., lower game periods, does not necessarily result in higher utilities for both players. For the simulation considering varying T^{D} whose $\sum \hat{U}_k^{\mathrm{D}}$ is shown in Fig. 9, we also see the difference in the recovered edges for the path graph in Figs. 11 and 12, where black dashed lines represent recovered edges, red dashed lines represent edges not recovered from normal attacks, black solid lines represent unattacked edges, and no lines represent edges attacked with strong attacks. In the case with $T^{\mathrm{D}} = 1$, the defender recovers only one edge for

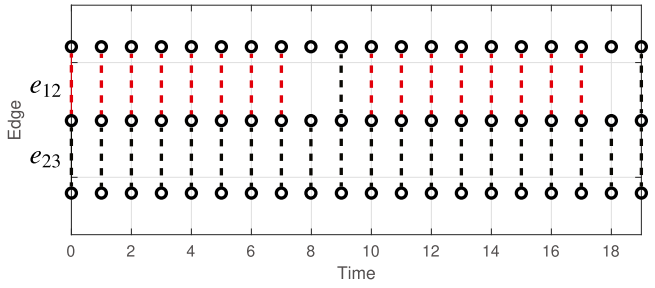

Fig. 11. Edges attacked and recovered with $T^{\mathrm{D}} = 1$.

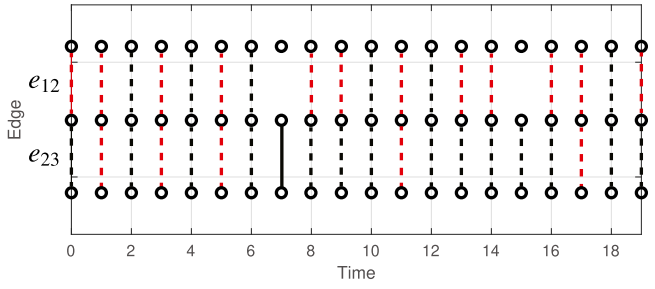

Fig. 12. Edges attacked and recovered with $T^{\mathrm{D}} = 2$.

most of the time, whereas in $T^{\mathrm{D}} = 2$ the defender recovers two edges at some k, resulting in a higher utility (as discussed in Lemma 2). This is because in the case with $T^{\mathrm{D}} = 1$, the defender always saves its energy to use it later, causing the recovery to be delayed. This yields a less connected graph $\mathcal{G}_k^{\mathrm{D}}$ over time since the defender tends to apply the recovery of fewer edges more consistently (rather than all edges at more time steps).

7. Conclusion

We have formulated a two-player game in a cluster forming of networks played over time. The players consider the impact of their actions on future network topologies, and adjust their strategies according to a rolling horizon approach. The players may have different computation capabilities represented by different horizon lengths and game periods. The performance of the players are measured by calculating the applied utilities, where in general, the player with a longer horizon length and a shorter game period performs better over longer intervals. We have confirmed that this is especially the case for more connected networks and when the attack/defense energy is more limited.

Declaration of Competing Interest

The authors declare that they have no known competing financial interests or personal relationships that could have appeared to influence the work reported in this paper.

References

[1] T. Alpcan, T. Basar, Network Security: a Decision and Game-Theoretic Approach, Cambridge University Press, 2010.
[2] A. Cetinkaya, H. Ishii, T. Hayakawa, Networked control under random and malicious packet losses, IEEE Trans. Autom. Control 62 (2017) 2434–2449.
[3] N. Charness, Search in chess: age and skill differences, J. Exp. Psychol. 7 (2) (1981) 467–476.
[4] J. Chen, C. Touati, Q. Zhu, A dynamic game approach to strategic design of secure and resilient infrastructure network, IEEE Trans. Inf. Forensics Secur. 15 (2020) 462–474.
[5] X. Gong, L. Duan, X. Chen, J. Zhang, When social network effect meets congestion effect in wireless networks: data usage equilibrium and optimal pricing, IEEE J. Sel. Areas Commun. 35 (2) (2017) 449–462.
[6] H. Ishii, Q. Zhu, Security and Resilience of Control Systems: Theory and Applications, Lecture Notes in Control and Information Sciences, 489, Springer, 2022.
[7] L. Jia, Y. Xu, Y. Sun, S. Feng, A. Anpalagan, Stackelberg game approaches for anti-jamming defence in wireless networks, IEEE Wireless Commun. 25 (2018) 120–128.
[8] M.L. Katz, C. Shapiro, Systems competition and network effects, J. Econ. Perspect. 8 (1994) 93–115.
[9] H. Li, W. Yan, Receding horizon control based consensus scheme in general linear multi-agent systems, Automatica 56 (2015) 12–18.
[10] Y. Li, C.A. Courcoubetis, L. Duan, R. Weber, Optimal pricing for peer-to-peer sharing with network externalities, IEEE/ACM Trans. Netw. 29 (1) (2021) 148–161.
[11] Y. Nugraha, A. Cetinkaya, T. Hayakawa, H. Ishii, Q. Zhu, Cluster formation in multiagent consensus via dynamic resilient graph games, in: Proc. IEEE Conf. Control Tech. App., 2021a, pp. 735–740.
[12] Y. Nugraha, A. Cetinkaya, T. Hayakawa, H. Ishii, Q. Zhu, Dynamic resilient network games with applications to multiagent consensus, IEEE Trans. Control Netw. Syst. 8 (2021b) 246–259.
[13] Y. Nugraha, A. Cetinkaya, T. Hayakawa, H. Ishii, Q. Zhu, Rolling horizon games for cluster formation of resilient multiagent systems, in: Proc. IEEE Conf. Dec. Control, 2021c, pp. 4829–4934.
[14] G.D. Pasquale, M.E. Valcher, Consensus for clusters of agents with cooperative and antagonistic relationships, Automatica 135 (2022).
[15] M. Pirani, E. Nekouei, H. Sandberg, K. Johansson, A graph-theoretic equilibrium analysis of attacker-defender game on consensus dynamics under $\mathcal{H}_2$ performance metric, IEEE Trans. Control Netw. Syst. 8 (2021) 1991–2000.
[16] H. Sandberg, S. Amin, K.H. Johansson, Special issue on cyberphysical security in networked control systems, IEEE Control Syst. Mag. 35 (2015) 20–23.
[17] T. Schouwenaars, J. How, E. Feron, Receding horizon path planning with implicit safety guarantees, in: Proc. American Control Conference, 2004, pp. 5576–5581.
[18] D. Senejohnny, P. Tesi, C. De Persis, A jamming resilient algorithm for self-triggered network coordination, IEEE Trans. Control Netw. Syst. 5 (2018) 981–990.
[19] Y. Shang, Resilient cluster consensus of multiagent systems, IEEE Trans. Syst. Man Cybern. Syst. 52 (2022) 346–356.
[20] M. Wang, Z. Wang, J. Talbot, J.C. Gerdes, M. Schwager, Game-theoretic planning for self-driving cars in multivehicle competitive scenarios, IEEE Trans. Robot. 37 (2021) 1313–1325.
[21] M. Zhu, S. Martinez, On the performance analysis of resilient networked control systems under replay attacks, IEEE Trans. Autom. Control 59 (3) (2014) 804–808.